

Giant dielectric behaviour of $\text{CaCu}_3\text{Ti}_4\text{O}_{12}$ subjected to post-sintering annealing and uniaxial stress

This article has been downloaded from IOPscience. Please scroll down to see the full text article.

2007 J. Phys.: Condens. Matter 19 236208

(<http://iopscience.iop.org/0953-8984/19/23/236208>)

View [the table of contents for this issue](#), or go to the [journal homepage](#) for more

Download details:

IP Address: 129.252.86.83

The article was downloaded on 28/05/2010 at 19:10

Please note that [terms and conditions apply](#).

Giant dielectric behaviour of $\text{CaCu}_3\text{Ti}_4\text{O}_{12}$ subjected to post-sintering annealing and uniaxial stress

Prasit Thongbai¹, Chivalrat Masingboon¹, Santi Maensiri^{1,4},
Teerapon Yamwong², Supattra Wongsanmai³ and Rattikorn Yimmirun³

¹ Integrated Nanotechnology Research Center (INRC) and Small & Strong Materials Group (SSMG), Department of Physics, Faculty of Science, Khon Kaen University, Khon Kaen, 40002, Thailand

² National Metals and Materials Technology Center (MTEC), Thailand Science Park, Pathumthani, 12120, Thailand

³ Department of Physics, Faculty of Science, Chiang Mai University, Chiang Mai, 50200, Thailand

E-mail: sanmae@kku.ac.th and santimaensiri@gmail.com

Received 21 March 2007, in final form 18 April 2007

Published 8 May 2007

Online at stacks.iop.org/JPhysCM/19/236208

Abstract

This paper reports the influences of the post-sintering annealing in argon and uniaxial compressive pre-stress on the giant dielectric properties of the $\text{CaCu}_3\text{Ti}_4\text{O}_{12}$ ceramics sintered at 1100 °C in air for 6 and 16 h. The $\text{CaCu}_3\text{Ti}_4\text{O}_{12}$ ceramic sintered at 1100 °C for 6 h exhibited high ϵ' of $\sim 1 \times 10^4$ whereas the $\text{CaCu}_3\text{Ti}_4\text{O}_{12}$ ceramic sintered at 1100 °C for 16 h possessed one order of magnitude higher dielectric constant ($\epsilon' \sim 2 \times 10^4$). The dielectric behaviour of both samples exhibits Debye-like relaxation, and can be explained based on a Maxwell–Wagner model. Post-sintering annealing in argon for 5 h leads to a significant increase in ϵ' for $\text{CaCu}_3\text{Ti}_4\text{O}_{12}$ ceramic sintered at 1100 °C for 16 h but a slight decrease in ϵ' for the $\text{CaCu}_3\text{Ti}_4\text{O}_{12}$ ceramic sintered at 1100 °C for 6 h. The ϵ' of the 16 h sintered $\text{CaCu}_3\text{Ti}_4\text{O}_{12}$ ceramic after annealing in argon increases with increasing temperatures, and exhibits a peak at about 150 °C, which is closely related to the oxygen vacancies. The dielectric behaviour of this argon-annealed sample follows the UDR law. The dielectric properties of the argon-annealed samples change significantly with the applied compressive stress (the absolute change can reach 25% at a maximum stress of 130 MPa). However, the changes in dielectric properties with the stress in the samples subjected to different sintering times follow opposing trends. The mechanisms responsible for this difference are discussed.

(Some figures in this article are in colour only in the electronic version)

⁴ Author to whom any correspondence should be addressed.

1. Introduction

Dielectric materials that have high dielectric constant and good thermal stability and are Ba/Pb free have particularly attracted ever-increasing attention for their practical applications in microelectronics such as capacitors and memory devices. Recently, calcium copper titanate ($\text{CaCu}_3\text{Ti}_4\text{O}_{12}$), a non-ferroelectric material with a cubic perovskite-related crystal structure, has generated considerable interest because it exhibits a giant dielectric constant of $\epsilon \sim 10^4$ for polycrystalline ceramics [1–8] and $\epsilon \sim 10^5$ for single crystals [9] in the kilohertz region over a large temperature range (from 100 to 600 K). This material does not undergo any structural change over the same temperature range, although its dielectric constant abruptly decreases to less than 100 below 100 K, showing a Debye-type relaxation [1, 2, 9]. It has also been reported [6] that the colossal dielectric constant of close to 10^6 at room temperature can be obtained in $\text{CaCu}_3\text{Ti}_4\text{O}_{12}$ after annealing in flowing argon at 1000°C for 6 h, and was attributed to the increase in concentration of oxygen vacancies and hence charge carriers. Fang and his co-worker [10] also studied the effects of post-annealing conditions on the dielectric properties of $\text{CaCu}_3\text{Ti}_4\text{O}_{12}$ thin films deposited on Pt/Ti/SiO₂/Si substrates by pulsed laser deposition. They observed that post-sintering annealing in nitrogen atmosphere produced strong low-frequency dielectric relaxation as the annealing temperature increases, whereas annealing in oxygen atmosphere at high temperature suppressed the relaxation and decreased the dielectric constant of the thin films. Most recently, the influence of post-sintering annealing on dielectric properties of $\text{CaCu}_3\text{Ti}_4\text{O}_{12}$ was further investigated by Wang and Zhang [11, 12]. They showed that the annealing treatments on $\text{CaCu}_3\text{Ti}_4\text{O}_{12}$ in reducing (nitrogen) and oxidizing (oxygen) atmospheres have significant changes in dielectric properties near room temperature. These results support the results reported in [6] and strongly suggest that the concentration of oxygen plays an important role in the dielectric properties of $\text{CaCu}_3\text{Ti}_4\text{O}_{12}$.

So far, several explanations for the origin of the colossal dielectric property of $\text{CaCu}_3\text{Ti}_4\text{O}_{12}$ material have been proposed to be due to either intrinsic or extrinsic effects. Since the giant dielectric response of this material was found to be very sensitive to the microstructure (such as grain size) and processing conditions (such as sintering temperature and time, cooling rate, and partial pressure) [3, 5–8], more investigations tend to indicate that the high dielectric constant originates from the extrinsic effect such as internal barrier layer capacitor (IBLC) [3–5], contact-electrode effect [13, 14], and special inhomogeneity of local dielectric response [15]. Although still unclear, the IBLC explanation of the extrinsic mechanism is widely accepted at the present stage [16–21].

In addition to its interesting dielectric property, $\text{CaCu}_3\text{Ti}_4\text{O}_{12}$ has remarkably strong linear current–voltage characteristics without the addition of dopants [22]. These excellent properties render this material particularly attractive for a wide range of applications. However, in some practical applications, dielectric ceramics may be subjected to mechanical or thermal stresses, causing changes in their properties. A prior knowledge of how the material properties change under different load conditions is therefore crucial for proper design of a device and for suitable selection of materials for a specific application. Despite this fact, material constants used in many design calculations are often obtained from a stress free measuring condition, which in turn may lead to incorrect or inappropriate device designs. However, the stress dependence of the permittivity in this highly dielectric material has not been thoroughly studied. It is therefore important to determine the properties of $\text{CaCu}_3\text{Ti}_4\text{O}_{12}$ material as a function of applied stress.

In the present study, we investigate the influences of the post-sintering annealing in argon and uniaxial compressive pre-stress on the giant dielectric properties of the $\text{CaCu}_3\text{Ti}_4\text{O}_{12}$ ceramics sintered at 1100°C in air for 6 and 16 h. The mechanisms responsible for the giant dielectric properties are discussed.

2. Experiment details

$\text{CaCu}_3\text{Ti}_4\text{O}_{12}$ powders were prepared by a conventional mixed oxide technique using the powders of CaCO_3 (99.95% purity; CERAC, USA), CuO (99.9% purity; CERAC, USA) and TiO_2 (99.5% purity; CERAC, USA). A stoichiometric mixture of the starting materials was ball-milled in ethanol for 24 h with a polyethylene bottle and zirconia balls. The mixed slurry was dried and then calcined at 950°C in air for 8 h. The calcined powders were ground and passed through a $106\ \mu\text{m}$ sieve to break up large agglomerates. Green bodies were prepared from the sieved powders using uniaxial pressing in a 16 mm die with an applied pressure of 100 MPa. The compacts were pressureless-sintered at 1100°C in air for 6 and 16 h. The final dimensions of the samples were ~ 12 mm in diameter and ~ 3 mm in height. A post-annealing process was carried out in flowing argon (99.999% purity) at 1000°C for 5 h. Throughout this paper, we assign symbols of CCTO-6 and CCTO-16 for the bulk samples of $\text{CaCu}_3\text{Ti}_4\text{O}_{12}$ sintered at 1100°C in air for 6 and 16 h, respectively, and assign symbols of CCTO-6–Ar and CCTO-16–Ar for the bulk samples of CCTO-6 and CCTO-16 after post-sintering annealing under flowing argon at 1000°C for 5 h.

The $\text{CaCu}_3\text{Ti}_4\text{O}_{12}$ ceramics were characterized by x-ray diffraction (XRD) (Philips PW3710, The Netherlands), and scanning electron microscopy (SEM) (LEO 1450VP, UK). The dielectric response of the samples was measured using a Hewlett Packard 4194A impedance gain phase analyser over the frequency ranges from 100 Hz to 1 MHz and at an oscillation voltage of 1 V. The measurements were performed over the temperature ranges from -30 to 160°C using an inbuilt cooling–heating system. Each measured temperature was kept constant with an accuracy of $\pm 1^\circ\text{C}$. Silver paint was coated on both surfaces of the samples and dried overnight. The dielectric properties of the samples after post-sintering annealing were measured under the influence of the compressive stress through spring-loaded pins connected to an LCZ-meter (Hewlett Packard 4276A) at the frequency of 1 kHz and room temperature (25°C). The details of the system are described in elsewhere [23].

3. Results and discussion

The microstructure of all the sintered ceramics revealed by scanning electron microscopy (figures 1(a) and (b)) shows polycrystalline grains with estimated grain sizes of 7.7 ± 1.9 and $9.0 \pm 1.9\ \mu\text{m}$ for CCTO-6 and CCTO-16. Figure 1(c) shows XRD patterns of the sintered ceramics before and after post-sintering annealing, confirming a main phase of $\text{CaCu}_3\text{Ti}_4\text{O}_{12}$ (JCPDS card no 75-2188) in all the samples. The values of lattice parameter a calculated from the XRD spectra are 0.7387 ± 0.00003 , 0.7385 ± 0.00004 , 0.7389 ± 0.00003 , and 0.7391 ± 0.00007 nm for CCTO-6, CCTO-16, CCTO-6–Ar, and CCTO-16–Ar, respectively. The values of a for CCTO-6 and CCTO-16 are slightly lower than the 0.7391 nm reported by Subramanian *et al* [1]. Post-annealing in argon results in an increase in the values of a for CCTO-6–Ar and CCTO-16–Ar, which are close to 0.7391 nm.

Figures 2(a) and (b) show the real and imaginary parts of dielectric dispersion for the samples of CCTO-6 and CCTO-16, measured using a Hewlett Packard 4194A impedance gain phase analyser at the frequency ranges from 100 Hz to 1 MHz with an oscillation voltage of 1 V at various temperatures. It is clearly seen from figure 2(a) that both samples exhibit the giant dielectric permittivity of $\sim 1 \times 10^4$ for CCTO-6 and $\sim 2 \times 10^4$ – 2.5×10^4 for CCTO-16 at low frequencies and each sample has a similar dielectric behaviour. First, all of the samples exhibit the Debye-like relaxation [2, 9, 14, 16]. This behaviour is similar to that observed in CCTO ceramics reported in the literature [3, 4, 7, 8, 17, 24, 25]. Second, ϵ' has little frequency dependence below the relaxation frequency. Third, the relaxation peak in both samples shifts to higher frequency at higher temperature.

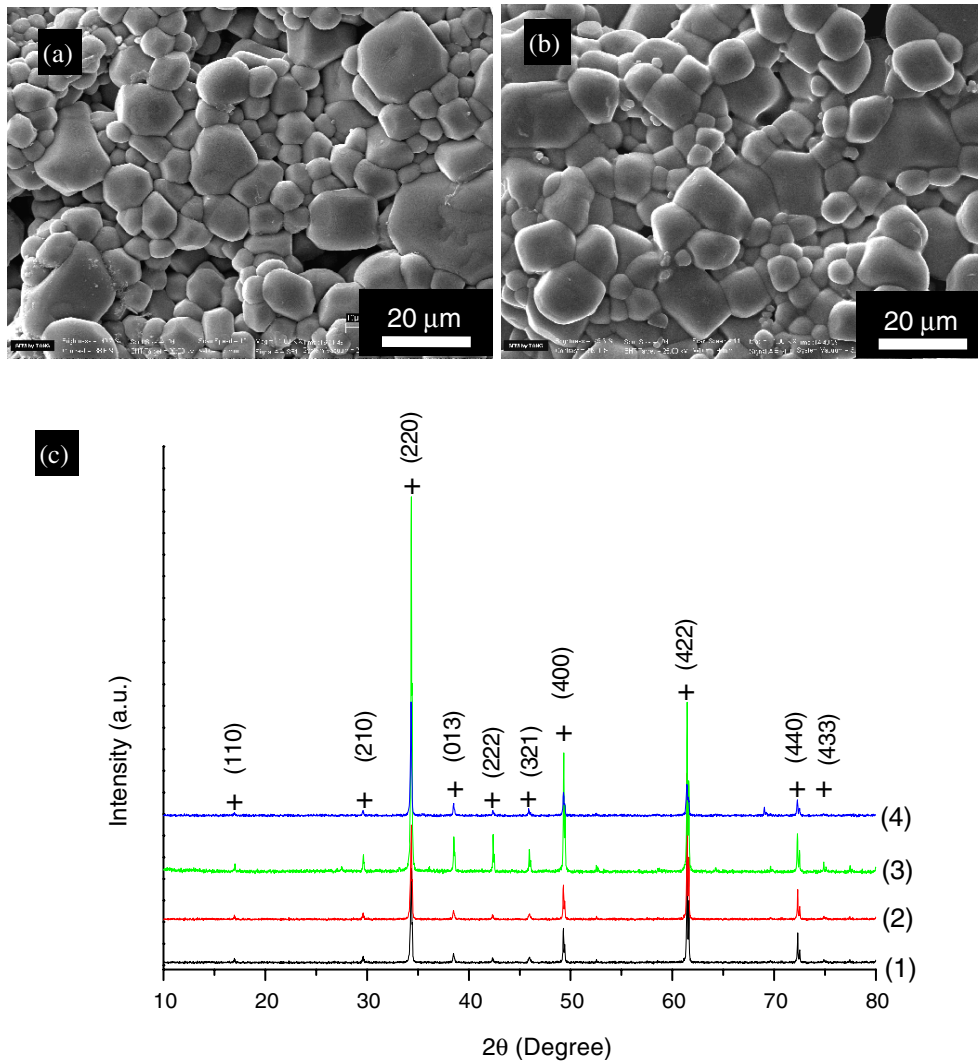


Figure 1. (a) and (b) SEM micrographs of sintered CCTO-6 and CCTO-16, respectively. (c) XRD patterns of the sintered materials of CCTO-6 and CCTO-16 before and after annealing at 1000 °C for 5 h under flowing argon. (1) CCTO-6, (2) CCTO-16, (3) CCTO-6–Ar, and (4) CCTO-16–Ar.

The Debye-like relaxation for CCTO-6 and CCTO-16 (figures 2(a) and (b)) can be fitted to the empirical Cole–Cole equation [26]:

$$\varepsilon^*(\omega) = \varepsilon'(\omega) - i\varepsilon''(\omega) = \varepsilon_\infty + [(\varepsilon_s - \varepsilon_\infty)/1 + (i\omega\tau)^\alpha] \quad (1)$$

where ε_s and ε_∞ are the static and high-frequency limits of the dielectric constant, respectively, τ is the most probable relaxation time, and α is a constant with values between zero and unity. For an ideal Debye relaxation $\alpha = 1$. If $\alpha < 1$, this implies that the relaxation has a distribution of relaxation times, leading to a broader peak shape than a Debye peak as shown in figure 2(b). The solid lines in figures 2(a) and (b) are the fitted results with $\alpha = 0.92$ for CCTO-6 and $\alpha = 0.91$ for CCTO-16. Figure 2(c) shows the plot of $\log \tau$ versus $1/T$, in which the solid line

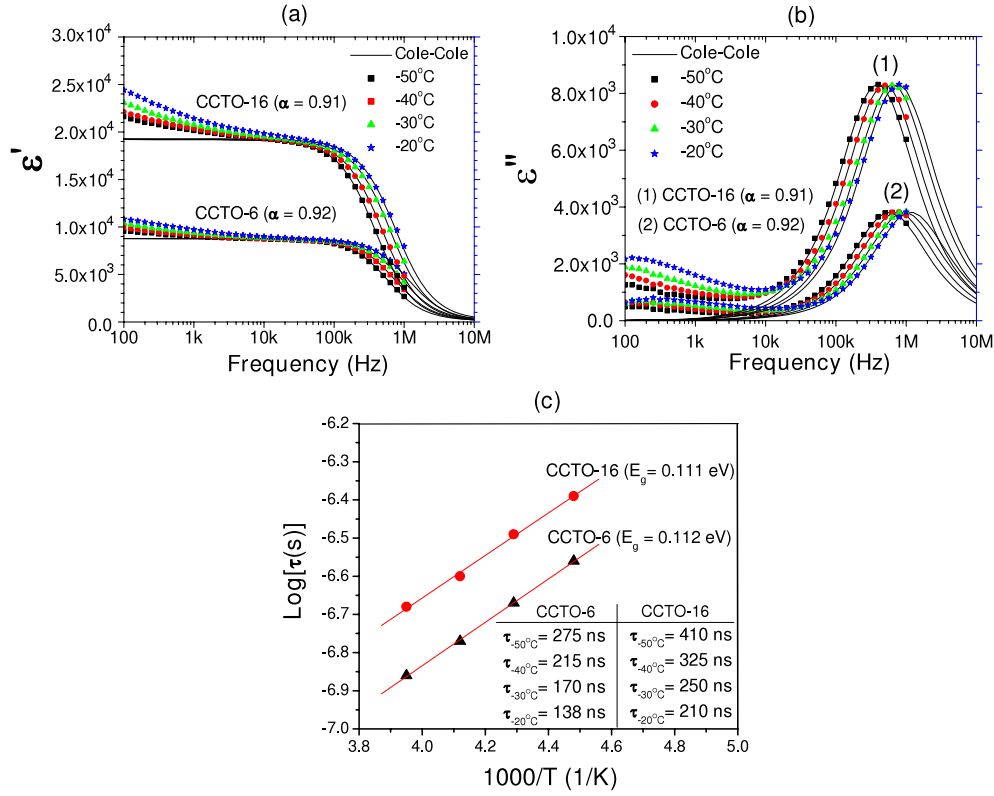


Figure 2. (a) Frequency dependence of the dielectric dispersion showing ϵ' at several temperatures for the sintered materials of CCTO-6 and CCTO-16. (b) Frequency dependence of the dielectric dispersion showing ϵ'' at several temperatures for the sintered materials of CCTO-6 and CCTO-16. (c) Arrhenius plot of dielectric relaxation time for the CCTO-6 and CCTO-16 samples. Solid lines in (a) and (b).

is the fitted result obeying the Arrhenius law, i.e.

$$\tau = \tau_0 \exp(E/k_B T) \quad (2)$$

where τ_0 is the pre-exponential factor, E is the activation energy for the relaxation, k_B is the Boltzmann constant, and T is the absolute temperature. τ is calculated from the relations $\omega\tau = 1$ and $\omega = 2\pi f_p$, where ω is the angular frequency and f_p is the characteristic frequency corresponding to the peak of ϵ'' . Activation energies of the low-frequency relaxation determined from the slopes of the graphs (figure 2(c)) were obtained to be 0.112 for CCTO-6 and 0.111 eV for CCTO-16. Both values are comparable to the reported values of 0.067 eV [16], 0.08 eV [3, 17], 0.093 eV [18], 0.059–0.076 eV [19], and 0.084–0.132 eV [7] for the grains of $\text{CaCu}_3\text{Ti}_4\text{O}_{12}$.

Since the dielectric response in both CCTO-6 and CCTO-16 shows the Debye-like relaxation which is approximately equal to the pure Debye functional form of a Maxwell–Wagner relaxation, the giant dielectric behaviour of both samples can be explained by using the Maxwell–Wagner relaxation model. The Maxwell–Wagner relaxation can be described by an equivalent circuit consisting of a series array of two subcircuits, one representing grain effects and one grain boundaries [8]. In each subcircuit, the resistor and capacitor are in parallel. From this equivalent circuit, the static permittivity (ϵ'_s) and dielectric relaxation time (τ) can

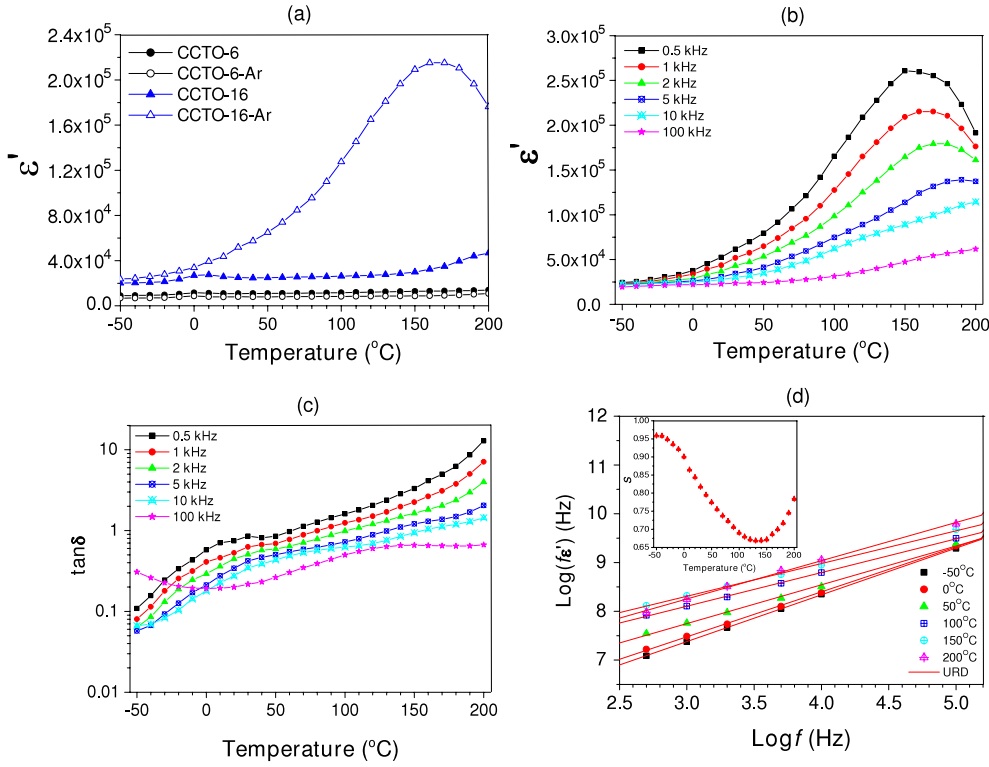


Figure 3. (a) Temperature dependence of ϵ' at frequency of 100 Hz for the sintered materials of CCTO-6 and CCTO-16 before and after annealing at 1000 °C for 5 h under flowing argon. (b) Temperature dependence of ϵ' at various frequencies for the CCTO-16 after annealing at 1000 °C for 5 h under flowing argon. (c) Temperature dependence of $\tan \delta$ at various frequencies for the CCTO-16 after annealing at 1000 °C for 5 h under flowing argon.

be calculated as

$$\epsilon'_s = (R_g^2 C_g + R_{gb}^2 C_{gb}) / [C_0 (R_g + R_{gb})^2] \quad (3)$$

and

$$\tau = [R_g R_{gb} (C_g + C_{gb})] / (R_g + R_{gb}), \quad (4)$$

where R_g , R_{gb} and C_g , C_{gb} are the resistance and capacitance of grains and grain boundaries, respectively [27]. Since $R_{gb} \gg R_g$, and C_{gb} is also much larger than C_g [3, 8], the effective dielectric permittivity (ϵ'_s) of the sample at frequencies much lower than the relaxation frequency $1/(2\pi\tau)$ can therefore be obtained approximately from equation (3),

$$\epsilon'_s = C_{gb} / C_0 \quad (5)$$

and we can approximate τ from equation (4) using

$$\tau \approx R_g C_{gb} = \tau_g (C_{gb} / C_g) \quad (6)$$

where $\tau = R_g C_g$ is the response time of the grains [8]. Since C_g and C_{gb} have been reported to be independent of temperature [3, 8], τ and τ_g have the same temperature dependence and the electrical response of grains has the same activation energy as that of the observed dielectric relaxation (figure 3(c)). On the basis of this analysis, we conclude that the activation

energies for the response of the grains in the samples of CCTO-6 and CCTO-16 are 0.112 and 0.111 eV, respectively. It is noted that the relation $\epsilon'_s = C_{gb}/C_0$ implies that ϵ'_s is determined only by the ratio between the grain boundary capacitance C_{gb} and the vacuum capacitance of the sample C_0 , and ϵ'_s is constant when C_{gb} is unchanged with temperature and frequency. Liu *et al* [28] observed a constant dielectric permittivity in wide temperature and frequency ranges in $\text{Bi}_{2/3}\text{Cu}_3\text{Ti}_4\text{O}_{12}$ because of its constant C_{gb} . Therefore, we attribute the differences in dielectric response observed in CCTO-6 and CCTO-16 to the differences in their grain boundary capacitances.

Figure 3(a) compares dielectric constant ϵ' of CCTO-6 and CCTO-16 before and after post-sintering annealing, showing a significant increase in ϵ' for the CCTO-16 after post-sintering annealing (CCTO-16–Ar) but a slight decrease in ϵ' for the CCTO-6 after post-sintering annealing (CCTO-6–Ar). The ϵ' of CCTO-16–Ar increases with increasing temperatures, and interestingly exhibits a peak at about 150 °C. This behaviour is important in explaining the effect of post-sintering annealing under a reducing atmosphere in the $\text{CaCu}_3\text{Ti}_4\text{O}_{12}$ system, and thus we further consider the dielectric behaviour of the CCTO-16 in detail. Figures 3(b) and (c) show temperature dependences of ϵ' and $\tan \delta$ over the frequencies of 500 Hz–100 kHz. ϵ' exhibits a peak around 150 °C (at 1 kHz) (figure 3(a)), whereas $\tan \delta$ increases near-exponentially with increasing temperature without a visible anomaly in the vicinity of 150 °C (figure 3(b)). This implies that the peak in ϵ' is not likely caused by the relaxation process. From figure 3(b), upon increasing the measured frequency, the peak position of ϵ' is shifted to higher temperatures and the peak height decreases, which is typical of a thermally activated Debye-like behaviour. The obvious upturn in $\tan \delta$ at low temperatures for the curves of high frequencies (at 100 kHz) shown in figure 3(c) is due to the relaxation widely studied before in the $\text{CaCu}_3\text{Ti}_4\text{O}_{12}$ system. This dielectric behaviour observed in CCTO-16–Ar is similar to that of the $\text{CaCu}_3\text{Ti}_4\text{O}_{12}$ sample after post-sintering annealing under nitrogen at 920 °C for 2 h, reported by Wang and Zhang [12]. In their report, the dielectric peak was observed at around 67 °C (340 K) (hereafter referred to as the 67 °C peak) and can be eliminated by annealing in oxidizing (O_2) atmosphere and created by annealing in reducing (N_2) atmosphere. This strongly suggests that the 67 °C peak is closely related to oxygen vacancies which made the grains of the $\text{CaCu}_3\text{Ti}_4\text{O}_{12}$ ceramic more conductive. Therefore, Wang and Zhang [12] proposed that the 67 °C peak was linked with the conductivity, the dielectric behaviour of the $\text{CaCu}_3\text{Ti}_4\text{O}_{12}$ after annealing in N_2 atmosphere followed the universal dielectric law (UDR) [29], and ϵ' can be calculated as

$$\epsilon' = [\tan(s\pi/2)\sigma_0 f^{s-1}]/\epsilon_0, \quad (7)$$

where σ_0 and the frequency exponent s are temperature dependent and ϵ_0 is the electric permittivity of free space. This equation can be rewritten as $f\epsilon' = A(T)f^s$ with the temperature-dependent constant $A(T) = \tan(s\pi/2)\sigma_0/\epsilon_0$. Hence, at a given temperature, a straight line with a slope of s should be obtained if $\log_{10}(f\epsilon')$ is plotted as a function of $\log_{10} f$. Since the URD-law model is typically valid for materials with hopping localized charge carriers, Wang and Zhang [12] confirmed that the charge carriers in the $\text{CaCu}_3\text{Ti}_4\text{O}_{12}$ after annealing in N_2 atmosphere are localized and not free charge carriers. This rules out the space-charge polarization as the origin of the 67 °C peak. To confirm this model, we plotted $\log_{10}(f\epsilon')$ as a function of $\log_{10} f$ for the CCTO-16–Ar as shown in figure 3(c). As expected, straight lines with slopes of s were obtained. The values of the parameter s deduced from linear fitting are presented in the inset of figure 3(c). It is seen from figure 3(c) that with increasing temperature the slope of the linear temperature dependence changes from a negative to a positive value at the transition temperature ~ 150 °C. This result is consistent with that observed in $\text{CaCu}_3\text{Ti}_4\text{O}_{12}$ after annealing in N_2 atmosphere with the transition temperature

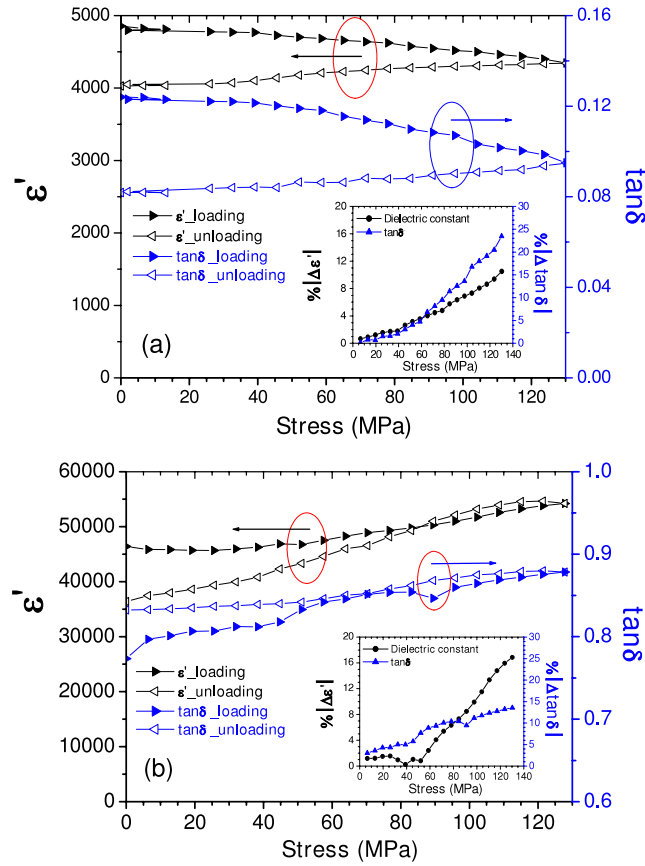


Figure 4. Uniaxial stress dependence of ϵ' and $\tan \delta$ at a frequency of 100 Hz for the samples of (a) CCTO-6 and (b) CCTO-16 after annealing at 1000 °C for 5 h under flowing argon.

at ~ 67 °C. The change in slope implies an alternation of the polarization mechanism [12]. According to our post-sintering annealing results, we conclude that the ϵ' peak is unlikely to be caused by a relaxation process. The ~ 150 °C peak is closely related to the oxygen vacancies and the dielectric behaviour follows the UDR law. Annealing the $\text{CaCu}_3\text{Ti}_4\text{O}_{12}$ sample in argon atmosphere at high temperatures would increase the concentration of the oxygen vacancies as obtained in the nitrogen-annealed $\text{CaCu}_3\text{Ti}_4\text{O}_{12}$ reported by Wang and Zhang [12].

Figures 4(a) and (b) show the stress dependent dielectric properties for CCTO-6–Ar and CCTO-16–Ar, respectively. It is clearly observed that the dielectric properties of both samples change significantly with the applied compressive stress (the absolute change can reach 25% at the maximum stress of 130 MPa). However, the changes in dielectric properties with the stress in the samples subjected to different sintering times follow opposing trends. For the CCTO-6–Ar, both ϵ' and $\tan \delta$ decrease with increasing stress, and, interestingly, continue to decrease upon the reduction of the applied stress (figure 4(a)). On the other hand, the dielectric properties of the CCTO-16–Ar sample increase when the stress is increased and decrease when the stress is gradually reduced, as shown in figure 4(b). To explain these observations, at least qualitatively, one needs to consider the different bases in the dielectric behaviours of the two ceramics. Clearly, the very high dielectric constant observed in CCTO ceramics is attributable to highly resistive grain boundaries [18, 30]. Interestingly, the CCTO-

16–Ar ceramic, which has been subjected to longer sintering (16 h), also possessed one order of magnitude higher dielectric constant, possibly due to higher concentration of the acceptor state (oxygen vacancies) available in the grain boundaries of the ceramic [31]. With lower concentrations of acceptor states, the CCTO-6–Ar should contain more mobile dipoles that can easily be activated by the applied stress. Hence, this leads to a stress-induced ageing mechanism, as reported previously [32–34], that results in the decrease in the dielectric constant and dielectric loss. This stress-induced ageing is irreversible, as the dielectric properties continue to decrease even upon reduction of the applied stress (figure 4(a)). On the other hand, in the case of the CCTO-16–Ar ceramic, with higher concentration of the acceptor states, there are competing mechanisms between the stress-induced ageing and the elastic deformation. Initially, with the stress-induced ageing mechanism still dominating, most of the acceptor states come to rest at the grain boundaries and stabilize the stress influence, as it is observed that the dielectric properties are rather stable at lower stress level [32–34]. A further increase in the compressive stress may result in a slight decrease in the grain boundary thickness. The effective dielectric properties of this ceramic, which can be regarded as the boundary layer capacitor (BLC) [16–21, 31], therefore increase, and the decrease in the effective dielectric properties follows with the reduction of the stress, as observed in figure 4(b).

4. Conclusion

The giant dielectric behaviour of polycrystalline $\text{CaCu}_3\text{Ti}_4\text{O}_{12}$ ceramics subjected to post-sintering annealing and under uniaxial stress was investigated. The dielectric behaviour of both CCTO-6 and CCTO-16 samples exhibits Debye-like relaxation, and can be explained based on the Maxwell–Wagner model. A significant increase in ϵ' was observed for the CCTO-16 after post-sintering annealing in argon (CCTO-16–Ar), whereas a slight decrease in ϵ' was observed for the CCTO-6 after post-sintering annealing in argon (CCTO-6–Ar). The ϵ' of CCTO-16–Ar increases with increasing temperatures, and interestingly exhibits a peak at about 150 °C. The ϵ' peak at 150 °C is unlikely to be caused by a relaxation process but is closely related to the oxygen vacancies. The dielectric properties of both CCTO-6–Ar and CCTO-16–Ar samples change significantly with the applied compressive stress, and this can be explained by the stress-induced ageing mechanism.

Acknowledgments

The authors would like to thank the Electron Microscopy Unit, Faculty of Science, Khon Kaen University, for providing SEM facilities. This work is supported by The Integrated Nanotechnology Research Center (INRC), Khon Kaen University, and The Postgraduate Education Development (PED) in Physics Program, The Commission on Higher Education, The Ministry of Education, Thailand.

References

- [1] Subramanian M A, Li D, Duan N, Reisner B A and Sleight A W 2000 *J. Solid State Chem.* **151** 323
- [2] Ramirez A P, Subramanian M A, Gardela M, Blumberg G, Li D, Vogt T and Shapiro S M 2000 *Solid State Commun.* **115** 217
- [3] Sinclair D C, Adams T A, Morrison F D and West A R 2002 *Appl. Phys. Lett.* **80** 2153
- [4] Adams T B, Sinclair D C and West A R 2002 *Adv. Mater.* **18** 1321
- [5] Fang T T and Shiao H K 2004 *J. Am. Ceram. Soc.* **87** 2072
- [6] Bender B A and Pan M J 2005 *Mater. Sci. Eng. B* **117** 339

- [7] Shao S F, Zhang J L, Zheng P, Zhong W L and Wang C L 2006 *J. Appl. Phys.* **99** 084106
- [8] Liu J, Sui Y, Duan C G, Mei W N, Smith R W and Hardy J R 2006 *Chem. Mater.* **18** 3878
- [9] Homes C C, Vogt T, Shapiro S M, Wakimoto S and Ramirez A P 2001 *Science* **293** 673
- [10] Fang L, Shen M and Cao W 2004 *J. Appl. Phys.* **95** 6483
- [11] Wang C C and Zhang L W 2006 *Appl. Phys. Lett.* **88** 042906
- [12] Wang C C and Zhang L W 2006 *Phys. Rev. B* **74** 024106
- [13] Lunkenheimer P, Bobnar V, Pronin A V, Ritus A I, Volkov A A and Loidl A 2002 *Phys. Rev. B* **66** 052105
- [14] Lunkenheimer P, Fichtl R, Ebbinghaus S G and Loidl A 2004 *Phys. Rev. B* **70** 172102
- [15] Cohen M H, Neaton J B, He L X and Vanderbilt D 2003 *J. Appl. Phys.* **94** 3299
- [16] Zhang L and Tang Z J 2004 *Phys. Rev. B* **70** 174306
- [17] West A R, Adams T B, Morrison F D and Sinclair D C 2004 *J. Eur. Ceram. Soc.* **24** 1439
- [18] Chiodeli G, Massarotti V, Capsoni D, Bini M, Azzoni C B, Mozzati M C and Lupotto P 2004 *Solid State Commun.* **132** 241
- [19] Capsoni D, Bini M, Massarotti V, Chiodelli G, Mozzatic M C and Azzoni C B 2004 *J. Solid State Chem.* **177** 4494
- [20] Kalinin S V, Shin J, Veith G M, Baddorf A P, Lobanov M V, Runge H and Greenblatt M 2005 *Appl. Phys. Lett.* **86** 102902
- [21] Fang T T, Mei L T and Ho H F 2006 *Acta Mater.* **54** 2867
- [22] Chung S, Kim I and Kang S 2004 *Nat. Mater.* **3** 774
- [23] Yimnirun R, Moses P J, Mayer R J and Newnham R E 2003 *Rev. Sci. Instrum.* **74** 3429
- [24] Aygun S, Tan X, Maria J P and Cann D 2005 *J. Electroceram.* **15** 203
- [25] Zhang J L, Zheng P, Wang C L, Zhao M L, Li J C and Wang J F 2005 *Appl. Phys. Lett.* **87** 142901
- [26] Cole K S and Cole R H 1941 *J. Chem. Phys.* **9** 341
- [27] Hippel V 1954 *Dielectrics and Waves* (New York: Wiley)
- [28] Liu J, Duan C, Yin W, Mei W N, Smith R W and Hardy J R 2004 *Phys. Rev. B* **70** 144106
- [29] Jonscher A K 1983 *Dielectric Relaxation in Solids* (London: Chelsea Dielectric Press)
- [30] Chen W P, Xiang W, Guo M S, You W C, Zhao X Z and Chan H L W 2006 *J. Alloys Compounds* **422** L9–12
- [31] Moulson A J and Herbert J M 2003 *Electroceramics* (Chichester: Wiley)
- [32] Yimnirun R, Ananta S, Ngamjarrojana A and Wongsanmai S 2006 *Curr. Appl. Phys.* **6** 520
- [33] Yimnirun R, Unruan M, Laosiritaworn Y and Ananta S 2006 *J. Phys. D: Appl. Phys.* **39** 3097
- [34] Yimnirun R 2006 *Int. J. Mod. Phys. B* **20** 3409